CHAPTER 2

Experimental Methods and Procedures

2. Experimental Methods and Procedures

2.1. Reagents and Apparatus

The used chemicals are Ammonium ceric nitrate $(NH_4)_2[Ce(NO_3)_6]$, anhydrous Ferric chloride ($FeCl_3$), β-Cyclodextrin ($C_{42}H_{70}O_{35}$), Sodium fluoride (NaF), 25% Ammonium solution (NH_4OH), Ammonium carbonate $[(NH_4)_2CO_3]$, Sodium hydroxide (NaOH), Sodium nitrate ($NaNO_3$), Potassium permanganate ($KMnO_4$), Hydrogen peroxide (H_2O_2), Hydrochloric acid (HCl), Nitric acid (HNO_3), Sulphuric Acid (H_2SO_4), Sodium sulphate (Na_2SO_4), Sodium hydrogen phosphate ($Na_2HPO_4,2H_2O$), Sodium bicarbonate ($NaHCO_3$). All chemicals and reagents used in this work were guaranteed reagent (G.R.) grade (Merck India, Mumbai). Graphite flakes used for preparation of Graphene oxide (GO) was Bought from Sigma Aldrich. The pH of any used solution was adjusted by the addition of 0.1 (M) HCl and NaOH solutions as per requirements. All glassware were washed with 15% HNO_3 solution and then thoroughly rinsed with double distilled water before use.

2.2. Preparation of Standard Solutions

2.2.1. Fluoride Solution

2.21 g of sodium fluoride was dissolved in one litre of double distilled water to prepare a Standard stock solution of fluoride (1000 $mg.L^{-1}$). The standard solution of fluoride was employed to achieve desired concentration of fluoride by appropriate dilution of the stock solution with fluoride free double distilled water.

2.2.2. Preparation of Phosphate Solution

1.87 g of $Na_2HPO_4 \bullet 2H_2O$ was dissolved in 1.0 L of double distilled water to prepare a Standard stock solution of phosphate (1000 $mg.L^{-1}$). Such standard solution of phosphate was then diluted as per requirement for respective experimental studies (Clesceri *et al*., 1998).

2.2.3. Preparation of Sulphate Solution

1.476 g of Na_2SO_4 was dissolved in 1.0 L of double distilled water to prepare a Standard stock solution of sulphate (1000 $mg.L^{-1}$).Dilution of standard stock solution was done requirement wise and applied to carry out analytical studies (Clesceri *et al.*, 1998).

2.2.4. Preparation of Bicarbonate Solution

1.37 g $NaHCO_3$ was dissolved in 1.0 L of double distilled water to prepare a Standard stock solution of bicarbonate (1000 $mg.L^{-1}$).The solution was standardized by acid base micro-titration using phenolphthalein as indicator and concentration of bicarbonate was determined as 1091.23 $mg.L^{-1}$ (Clesceri *et al.*, 1998).

2.2.5. Preparation of Chloride Solution

1.647 g of dried NaCl was dissolved in 1.0 L double distilled water to prepare a Standard stock solution of chloride (1000 $mg.L^{-1}$) (Clesceri *et al.*, 1998).

2.3. Analytical Processes

2.3.1. Fluoride Analysis

Concentration of fluoride in water samples were analysed by ion selective electrode (Hach made, USA, fluoride ion detection limit ranging between 1-1900 $mg.L^{-1}$). Here, 25 mL of filtrate was taken in glass beaker and a fluoride adjustment buffer powder (Hach made) was dissolved in solution to adjust solution pH in range of 5.0-5.8. Fluoride concentration of respective solution was then analysed by duly calibrated ion selective electrode.

2.3.2. Hardness Estimation (Titrimetric method)

Reagents: (i) 0.01(M) EDTA solution, (ii) ammonium chloride and ammonium hydroxide buffer (pH-10.0), (iii) Eriochrome Black-T as indicator.

Procedure: 50 mL sample was taken into 250 mL conical flask. 2.0 mL buffer solution was added to sample to maintain pH within range of 9 to 10.This solution was then titrated with 0.01(M) EDTA using Eriochrome Black-T as indicator up to a clear blue solution indicating end point (Clesceri *et al.*, 1998).

2.3.3. Total Dissolved Solid (TDS)

Well mixed definite volume of water sample was filtered with whatman-42 filter paper of exactly known weight. The filtrate was collected in a preheated porcelain crucible of known weight. Then filtrate was evaporated on a water bath and dried to a constant weight at 180°C inside a muffle furnace. After desiccation at room temperature for one hour, it was again weighted and the increase of weight was due to TDS (Clesceri *et al.*, 1998).

2.3.4. Estimation of pH_{ZPC}

The point of zero charge (pH_{zpc}) of the adsorbent was analysed by pH metric method used by *Babic et al.* (Babić *et al*., 1999). Each 50 mL of 0.1(M) KNO_3 solution was adjusted from 3.0 to 10.0 sequentially by adding either fixed strength of HCL (0.01M) or (0.01M) NaOH using a pH meter. Then 0.01g of adsorbent was taken in 250 mL polyethylene (PE) bottle which was securely capped immediately. The bottles were then placed within a thermostatic shaker and agitated at 250 (± 5) rpm and shaken for 48 h. The pH values of the supernatant liquid were noted after 48 h. The value of pH_{zpc} could be found from the curve that cuts the line of pH_i of the plot of ΔpH versus pH_i (Babić *et al*., 1999).

2.4. Instrumental and Software Used

Shaking of all batch experiments was carried out in temperature and speed controlled shaker. pH was measured by a pH electrode (Hach made, USA). A high precision electrical balance has been used for all weighing. SPSS-17 (SPSS Inc., Chicago, USA), Neuro solution 5®, Design-Expert (Stat-Ease Inc.,version7.0.3, Minneapolis, USA) and Origin Pro 8 (Origin Lab corporation, Northampton, USA) software were applied for data analysis and fitting the values in various models.

2.5. Synthesis of Proposed Adsorbents

2.5.1. Preparation of Ce(IV)- Incorporated Hydrous Fe(III) Oxide Named as (CIHFO), HFO and HCO

The method of preparation of hydrous cerium (IV)-incorporated iron (III) oxide followed the co-precipitation method under ambient laboratory environment. The concentration of ferric chloride (0.1M) solution in 0.1M HCl was kept constant while the concentration of ammonium ceric nitrate in 0.1M HNO_3 was varied in different molar levels. Both solutions were mixed together and the pH of the mixture was increased to ~ 6.0-7.0 by drop wise addition of ammonia solution (mixture of 25% ammonia solution and 0.1 M ammonium carbonate solution). The brownish yellow gel like precipitate was developed and was left for aging for 24 h. The precipitate was filtered through 0.45 μm membrane filter and washed repetitively with double distilled water to remove impurities. The residue was dried at 75°C (± 5°C) in an air oven. The hot mass immediately after drying was treated with cold water to break down it into small particles. The air dried particles were ground and sieved in between 50 and 100 mesh for collecting the particles of size ranged between 140-290 μm, and used for the conducting the batch and column experiments respectively. Preparation of HFO and HCO followed same synthesis pathway using anhydrous ferric chloride (0.1M) solution in 0.1M HCl and ammonium ceric nitrate in 0.1M HNO_3 for preparation HFO and HCO respectively. Others steps were similar with CIHFO preparation.

2.5.2. Surface Modification of Ce(IV) - Incorporated Hydrous Fe(III) Oxide (CIHFO) with Graphene Oxide and Named as GO-CIHFO

2.5.2.1. Preparation of Graphene Oxide (GO)

Synthesis of Graphene oxide was based on the modified Hummer's method (Hummers and Offeman, 1958). In this study, an exactly known amount of graphite flakes (3.0 g) was mixed with 50% weight amount of $NaNO_3$ (in present experiment, 1.5 g) and concentrated H_2SO_4 (75 mL, generally 25 times higher than the volume of graphite weight amount) was added to the mixture and stirred it at 0°C in ice bath. For 6 h of experiment, $KMnO_4$ (9.0 g) was added in portion after certain interval under vigorous stirring so that the temp should not exceed 20°C. A pasty light brownish mixture was developed and then additional $KMnO_4$ (9.0 g) was added to it and stirred it for 12 h at room temperature.

Then 300 mL of ice chilled distilled water was added slowly to the mixture followed by drop wise addition of 30% H_2O_2 to reduce the excess $KMnO_4$ to control further oxidation. With the passing of time as the reaction continued, the suspension turned brown to light yellow. This mixture sequentially washed with 5% of HCl and warm water thoroughly to remove impurities and obtained mass was dried and dispersed in distilled water. After that it was centrifuged at 5000 rpm for 30 min to remove large heavy particles. The supernatant was filtered through 0.45 μm pore size membrane and washed with 50% ethanol to isolate graphene oxide mass and was dried under vacuum at 60°C and collect pure GO as a brownish black solid product.

2.5.2.2. Preparation of Graphene Oxide Tweaked Ce(IV) - Incorporated Hydrous Fe(III) Oxide (GO-CIHFO)

Different qualitative of mass weight percentage of prepared GO (**Table-*2.1***) was taken separately in Erlenmeyer flasks and sonicated about 30 h, in mixed solution (1:1 v/v) of (0.1M) ferric chloride in (0.1M) HCl and (0.05M) ammonium ceric nitrate in (0.1M) HNO_3 for complete dispersion. Then pH of the mixture with well dispersed GO suspension was increased to ~6.0-7.0 by drop wise addition of ammonia solution (mixture of 25% ammonia solution and 0.1 M ammonium carbonate solution). Blackish-brown Jelly like precipitated mass obtained was kept as such with the mother liquid for overnight, and then filtered, washed simultaneously with double distilled water and oven dried at 50-55°C. Finally, the composite was crushed and sieved to obtain the desired particle size (140-290μm) and kept for further analytical experiments.

Table- 2.1: Ingredients used for preparation of GO incorporated CIHFO (GO-CIHFO)

S. No.	% of GO in composite	Required Amount of GO (g)	0.1(M) $FeCl_3$ (mL)	0.05(M) $Ce(NH_4)_2(NO_3)_6$ (mL)
1.	Blank	-	100	100
2.	5	0.0967	100	100
3.	10	0.204	100	100
4.	15	0.3245	100	100
5.	20	0.4597	100	100
6.	25	0.613	100	100

2.5.3. Synthesis of β-cyclodextrin modified Ce(IV) - Incorporated Hydrous Fe(III) Oxide (βC-CIHFO)

The synthetic pathway for βC-CIHFO preparation is similar to the preparation process of GO-CIHFO. For the preparation of β-CD modified Ce (IV)-incorporated hydrous Fe(III) oxide (βC-CIHFO), β-CD with different molar solutions were mixed with the preselected molar ratio of 1.0 : 0.5 of $FeCl_3$ and $[(NH_4)_2\,[Ce(NO_3)_6]$ mixture followed by pH neutralisation at 7.0, after 24 h of aging followed by membrane filtration process, drying and sieving have been done. Complex of β-CD incorporated CIHFO composites was formed in such a manner using simple co-precipitation method. The synthesized nanocomposites were optimized for the removal efficiency of fluoride and the maximum efficiency was achieved for the molar composition of β-CD: Fe: Ce as 0.04:1.0:0.5 and used for rest of the batch experimental studies.

2.6. Adsorbent Characterisation

2.6.1. Surface Morphology Study

2.6.1.1. Optical Microscope and Scanning Electron Microscope (SEM) Study with EDX Analysis.

The optical microscope or light microscope, is a type of microscope, commonly uses visible light and a system of lenses to magnify images of small objects. Images obtained from an optical microscope can be captured by either normal or photosensitive cameras to create a micrograph. Purely digital microscopes are now used equipped with CCD camera to examine any kind of sample and screening the resulting image done directly on a computer screen without the need for eyepieces. NICON Eclipse LV100POL trinoculer optical

microscope with CCD camera has been used for characterisation of all three adsorbents.

A scanning electron microscope (SEM) is an advanced electron microscope that can effectually scanned surface of any material with a focused beam of highly energetic electrons to produces images. Interaction of electrons with atoms in the sample produces various signals that contain information about the surface topography and composition of the sample. The electron beam is generally scanned in a raster scan pattern, and the beam's position is combined with the detected signal to produce an image. SEM can resolve higher magnifications than optical microscopes. SEM can achieve resolution better than 1 nm. Samples are observed in high vacuum in conventional SEM, or in low vacuum or wet conditions in variable pressure or environmental SEM, and at a wide range of cryogenic or elevated temperatures with specialized instruments. When samples are probed with focused electron beams, a variety of signals produced by a SEM includes secondary electrons, back–scattered electrons, characteristic x–rays, light (cathode-luminescence), sample current and transmitted electrons. Secondary electron detectors are standard equipment in all SEMs, but it is rare that a single machine would have detectors for all possible signals. The number of secondary electrons is a function of the angle between the surface and the beam. On a flat surface, the plume of secondary electrons is mostly contained by the sample, but on a tilted surface, the plume is partially exposed and more electrons are emitted. By scanning the sample and detecting the secondary electrons, an image displaying the tilt of the surface is created. SEM analyses are conducted in vacuum environments. All non– conductive samples are usually coated with electrically conductive

coatings before they are observed in SEM. In the present study, SEM characterization of the adsorbents was performed by a Hitachi, S–530 (Make: Elko Engineering, Ltd., Japan) scanning electron microscope.

2.6.1.2. Transmission Electron Microscope (TEM) with EDX Analysis

Transmission electron microscopy (TEM), is a microscopic technique that allows a beam of electrons to be transmitted through a specimen to form an image. The produced image is then magnified and focused onto an imaging device to form images of a significantly higher resolution than light microscopes, owing to the smaller de Broglie wavelength of electrons. This enables the instrument to capture fine detail—even as small as a single column of atoms, which is thousands of times smaller than a resolvable object seen in a light microscope.

Transmission electron microscopic (TEM-'TECNAI G2 30 ST', FEI, Netherlands) images were recorded at different magnifications. The samples for the TEM were suspended in 0.25 % Vinylec-E chloroform solution by sonication, and one drop of the suspension was casted onto a carbon film coated copper grid and dried under IR lamp. It was then mounted on the Double Tilt Specimen Holder to perform TEM analysis.

2.6.1.3. Atomic Force Microscope (AFM) Study

Atomic force microscopy (AFM) is a kind of very-high-resolution scanning probe microscopy (SPM), with demonstrating resolution on the order of fractions of a nm, more than 1000 times better than the optical diffraction limit. AFM can be used to form an image of the three-dimensional shape

(topography) of a sample surface at a high resolution. This is achieved by raster scanning the position of the sample with respect to the tip and recording the height of the probe that corresponds to a constant probe-sample interaction. The surface topography is commonly displayed as a pseudo colour plot. Atomic force microscopic (AFM) images were taken by Innova Atomic Force Microscope (Bruker AXS Pte Ltd) using optical beam deflection to monitor the displacement of a micro-fabricated silicon cantilever having a spring constant of 80 Nm^{-1} to visualize the topography of the mixed oxide surface.

2.6.1.4. Surface Area Analysis

The Brunauer–Emmett–Teller (BET) gas adsorption theory is the fundamental backbone for the measurement of surface area in highly porous composite. The procedure depends upon tracing out the volume amount of a gas required to form unimolecular adsorbed layer (monolayer) on the solid. According to this theory, multilayer formation in any adsorption process is the true picture of physical adsorption where pressure and thermal energy play a crucial role. When system exhibits low pressure gaseous molecules would possess high thermal energy and high escape velocity, hence less number of gaseous molecules would be available near the surface of adsorbent resulting monolayer adsorption. In reverse condition, with high pressure and low temperature, thermal energy of gaseous molecules decreases and more and more gaseous molecules would be available per unit surface area and hence multilayer adsorption would occur(Brunauer *et al*., 1938). Nowadays The BET theory is extensively applied to determine the surface area of any composite and expressed as:

$$V_{total} = \frac{V_m C\left(\frac{P}{P_0}\right)}{\left(1-\frac{P}{P_0}\right)\left(1+C\left(\frac{P}{P_0}\right)-\frac{P}{P_0}\right)} \qquad \textit{(Eq.2.1)}$$

Where V_{total}= the volume of gas adsorbed under pressure P, P_0= saturated vapour pressure at the same temperature. V_m= the volume of gas adsorbed when the surface is covered with a monolayer and c = constant for a given adsorbate.

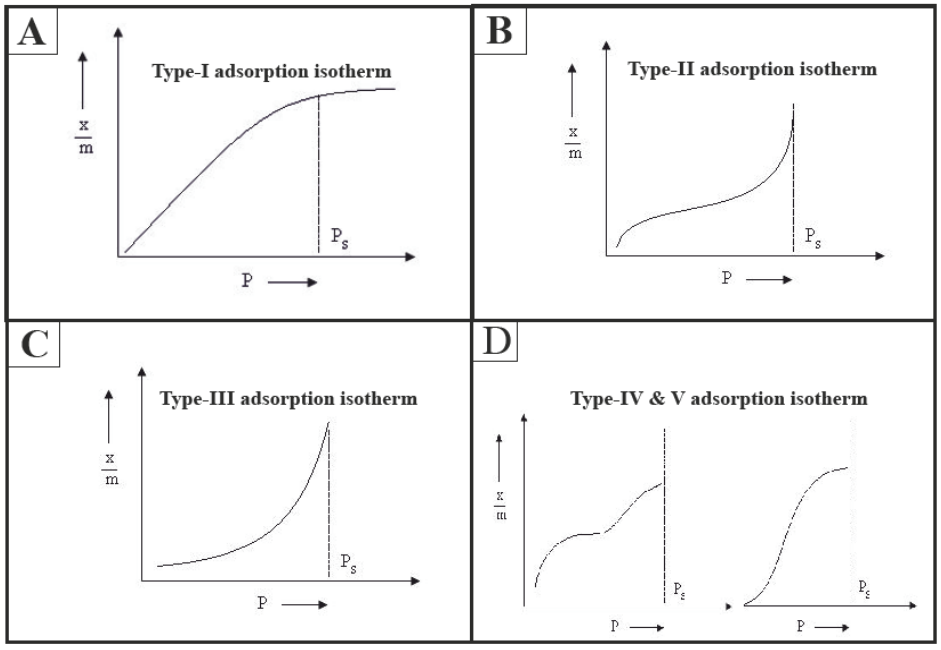

Fig.2.1: (A-D) express five different types of graphs with their unique characteristics to identify the pattern of adsorption isotherm by BET theory

Five different types of graphs and their characteristics are used extensively in recent days to explain and identify graphically the pattern of adsorption isotherm by BET theory (fig.2.1). Type I and Type II Adsorption Isotherm lead to monolayer formation. Both Type II and Type III Adsorption Isotherm exhibit strong nonconformity in respect Langmuir adsorption model.

Intermediate flat region of the Type II adsorption isotherm graph resembles to monolayer formation whereas Type III Adsorption Isotherm explains the formation of multilayer firmly. In both cases of type IV and type V adsorption isotherm, at lower pressure region of graph is quite similar to Type II. This explains formation of monolayer followed by multilayer (Brunauer *et al*., 1938).

2.6.2. X-ray Powder Diffraction (XRD) Analysis

X-Ray Diffraction Analysis (XRD) investigates crystalline material structure, including atomic arrangement, crystallite size, and imperfections. X-ray diffraction (XRD) patterns of all three proposed adsorbents were recorded using an X-ray diffractometer (Philips Analytical PW-1710) equipped with Cu-Kα radiation (λ=1.5418 Å) at a scanning speed 0.4° min-1 between the °2Θ = 10 and 70 operated at voltage 40 kV and applied potential current 30 mA.

2.6.3. Thermogravimetric (TG) and Differential Thermal Analysis (DTA)

TG and DTA spectra for all three proposed adsorbents were recorded using Setaram analyser in inert gas atmosphere with a heating rate of 20°C min^{-1} over a temperature range 50°C to 1200°C to find out degree of thermal stability and also detect the possibility of any phase transformation of the oxide associated with increasing temperature of heat treatment.

2.6.4. Infrared (IR) Spectroscopy Study

Infrared (IR) spectrometer generally used to measures the absorption of IR radiation by any materials. The molecule, which shows change in dipole

moment during the vibrations are absorb the IR radiation and shows the resonance. These resonance frequencies (equal to vibrational frequency) are characteristic of functional groups present in a molecule. This technique widely used for routine identification of functional groups existing within any analysing mixtures or compounds. The infrared region of the electromagnetic spectrum may be roughly categorised into three main sections: Near–infrared (overtone region): 0.8–2.5 μm (12500–4000 cm^{-1}); Middle–infrared (vibration–rotation region); 2.5–50 μm (4000–200 cm^{-1}) and Far–infrared (rotation region): 50–1000 μm (200–10 cm^{-1}). Among these three zone, middle IR region that is from 2.5 to 25 μm i.e., wavenumber 4000 to 400 cm^{-1} is broadly applicable for analytical purpose.

When any sample material is irradiated by IR radiation along with appropriate frequencies; all atoms, ions, and functional groups present in molecules will vibrate about their bonds and energy will be absorbed. Each bending and stretching vibrational mode of a particular molecule or functional group will definitely absorb at a particular frequency. With exposure to appropriate IR frequencies, energy will be absorbed from the incident radiation as vibration intensities increase. Similarly, many IR frequencies have no such effect at all and will not be absorbed. For the study, IR characterization of the proposed adsorbents were carried out with Fourier transform infrared spectrophotometer (Perkin–Elmer, FTIR, Model–RX1 Spectrometer, USA) in the range of 400–4000 cm^{-1}. Adsorbents samples were prepared in the forms of potassium bromide (KBr) disk. The adsorbents in the form of powder or finely divided states were ground with 200 mg of KBr (spectroscopic grade) in a mortar and

pressed into 10 mm diameter disks under 10 tons of pressure and high vacuum for FTIR analysis.

2.6.5. Raman Spectroscopy Study

Raman spectroscopy is a complementary advanced technique of IR, is commonly used in to provide a functional group (shows change in polarizability during the vibration of functional group) fingerprint of any chemical composite by which molecules can be identified. It count on inelastic scattering, or Raman scattering, of monochromatic light, usually from a laser in the visible, near infrared, or near ultraviolet range. The laser light interacts with molecular vibrations, phonons or other excitations in the system, resulting in the energy of the laser photons being shifted up or down. Such the shift in energy gives information about the vibrational modes in the system.

2.6.6. X-ray Photoelectron Spectroscopy (XPS) Study

X-ray photoelectron spectroscopy (XPS), a unique surface-sensitive quantitative spectroscopic measurement technique that can quantity the detailed elemental composition, empirical formula, chemical state and electronic state of all the elements present within a material. XPS spectra are obtained by irradiating a material with a beam of X-rays while simultaneously measuring the kinetic energy and number of electrons that escape from the top 0 to 10 nm of the material being analysed. XPS requires high vacuum or ultra-high vacuum conditions. Here, the X-ray photoelectron spectroscopy (XPS) measurements are done using an OMICRON-0571 system.

2.7. Experimental Design for Batch Study

A systematic batch adsorption study is essential step to establish an adsorbent as a good water purifier. To evaluate the effect of different parameters (initial solution pH, adsorbent dose, initial fluoride concentration, temperature, contact time, co-existing ions etc.) a series of batch adsorption process was carried out by mechanical agitation. A measured volume fluoride solution (50 mL / 100 mL) with desired initial fluoride concentration (C_i, $mg.L^{-1}$) was taken in 250 mL polyethylene (PE) bottle along with a certain mass (0.01 g / 0.05 g) of adsorbent (except dose variation study) and agitated at 250 (± 5) rpm using a thermostatic shaker at adjusted temperature (except temperature dependent experiment) for two hours (except time dependent experiment). The filtrate obtained by immediate filtration process was analysed to evaluate residual concentration of fluoride (C_f, $mg.L^{-1}$).The adsorbed amount of fluoride by adsorbent was calculated by application of the following mass balance equation(Eq. 2.2) (Biswas *et al*., 2009; Ghosh *et al*., 2014; Mukhopadhyay *et al*., 2017):

$$\boldsymbol{Q_e = \left(C_i - C_f\right) \times \frac{V}{M}} \qquad \textit{(Eq. 2.2)}$$

Where Q_e is the adsorption capacity ($mg.g^{-1}$), V the volume of solution (L), M is the mass of adsorbent (g) used to carry out the batch experiments. The significance of C_i and C_f have been given previously.

The removal percentage of fluoride by adsorbate was calculated (Podder and Majumder, 2016) as follows:

$$\boldsymbol{Regeneration(\%) = \frac{(C_i - C_f)}{C_i} X\ 100} \qquad \textit{(Eq. 2.3)}$$

2.7.1. Adsorption Kinetics Study

Experiments on fluoride adsorption kinetics were initiated by batch adsorption study at neutral pH (7.0±0.2) in a temperature controlled shaker with agitation speed at 250 (± 5) rpm with varying concentration and temperature. pH of adsorbate solution was measured by pH meter (Hach made, USA) followed by addition of 0.1 (M) NaOH or 0.1 (M) HCl for pH neutralisation for continuous experimental run. Reaction mixture was withdrawn at a predetermined time interval from the start to till the equilibrium plateau was reached. All collected sample solutions then were filtered using 0.45 μm pore size membrane filter and filtrates were analysed for residual fluoride measurement by an ion selective electrode. The adsorption capacity (Q_t, $mg.g^{-1}$) at any time, t (min.) was calculated using the equation (2.4) (Biswas *et al*., 2009; Ghosh *et al*., 2014; Mukhopadhyay *et al*., 2017),

$$\boldsymbol{Q_t = (C_i - C_t) \times \frac{V}{M}} \qquad \textbf{\textit{(Eq. 2.4)}}$$

Where, C_t is fluoride concentration ($mg.L^{-1}$) at any time, t and other terms of equation (2.3) have their own significance and given elsewhere.

2.7.1.1. Adsorption Kinetics Modeling

Adsorption of any pollutant by any adsorbent is time dependant. Physico-chemical nature of adsorbent also influences the overall adsorption process. Kinetics modeling for batch adsorption process is considered very crucial aspect as it helps to determine the adsorption mechanism and also help in explore to rate determining step of ongoing adsorption process. In present batch study, Pseudo-first order, Pseudo-second order, Mass transfer, Intra-

particle diffusion, Elovich Model and Richenberg model applied to study different kinetics parameters.

2.7.1.1.1. Pseudo First Order Kinetics Equation

The Lagergren pseudo first -order kinetics equation (Biswas *et al*., 2009; Kumar *et al*., 2005) for any adsorption process involved in between liquid-solid phase is based on solid uptake capacity. As per this model, the whole adsorption rate is directly proportional to the difference exist in-between the saturation concentration and the amount of solute uptake with time.

In general, the equation is expressed as:

$$\frac{dQ_t}{dt} = k_1(Q_e - Q_t) \qquad \textit{(Eq. 2.5)}$$

Where Q_e and Q_t are the amounts of pollutant adsorbed per unit weight of adsorbent ($mg.g^{-1}$), i.e. uptake capacity at equilibrium and at time t (min), respectively and k_1 stands for equilibrium rate constant for pseudo-first order adsorption.

While integrating the equation 2.4 applying boundary conditions t = 0 to t = t and Q_t = 0 to Q = Q_t, the linear form of equation as follows:

$$log\,(Q_e - Q_t) = logQ_t - \frac{k_1}{2.303}t \qquad \textit{(Eq. 2.6)}$$

The non-linear form of the pseudo-first-order kinetic model equation can be expressed as follows:

$$Q_t = Q_e\{1 - exp^{(-k_1.t)}\} \qquad \textit{(Eq.2.7)}$$

This linear form of pseudo-first-order kinetic model equation, usually applicable for experimental data but generally differs from a true first order equation in following manners:

Numbers of available sites cannot be expressed by the parameter$(Q_e - Q_t)$.

log (Q_e) is considered as an adjustable parameter and it is often observed that the intercept is not equal to log(Q_e) in respect of plot $log\ (Q_e - Q_t)$ versus time, t (min.).Henceforth application of nonlinear form of pseudo-first-order kinetic model equation is thought to be more appropriate for interpretation of experimental data.

2.7.1.1.2. Pseudo-Second Order Kinetics Equation

Pseudo second order kinetics model as described by Ho and McKay (Ho and McKay, 1999) (Eq.2.8) assumes that chemisorption is controlling the adsorption rate by sharing or exchanging of electrons in between adsorbent and adsorbate. The equation is expressed as;

$$\frac{dQ_t}{dt} = k_2(Q_e - Q_t)^2 \qquad \textit{(Eq.2.8)}$$

Here, k_2 stands for equilibrium rate constant for Pseudo-second order kinetic reaction ($g.mg^{-1}.min^{-1}$), where Q_e and Q_t have same significance as given above. Integrating the equation 2.7, with boundary conditions t = 0 and $Q_t = 0$ to t = t and $Q = Q_t$, the equation becomes:

$$\frac{1}{(Q_e - Q_t)} = \frac{1}{Q_e} + k_2 t \qquad \textit{(Eq.2.9)}$$

After rearrangement, the non-linear expression of Pseudo-second order kinetic Model can be expressed as follows:

$$Q_t = \frac{(t.k_2.Q_e^2)}{\{1+(t.k_2.Q_e)\}} \qquad \textit{(Eq. 2.10)}$$

Analysis of experimental data from plot Q_t versus t by the equation (2.9) the values of Q_e and k_2 can be obtained.

2.7.1.1.3. Mass Transfer

Extent of removal of any pollutant by adsorption process highly influenced by wide range of contaminants transfer from bulk solution to the surface of the solid adsorbent and at the interface of particular adsorbent or at the interface of liquid and solid particles. For the present studies this probability was examined by using *Mckay et al.* model (McKay *et al*., 1981).

$$\ln\left(\frac{C_t}{C_i} - \frac{1}{1+mk}\right) = \ln\left(\frac{mk}{1+mk}\right) - \left(\frac{1+mk}{mk}\right)\beta_1 S_s\, t \qquad \textit{Eq. 2.11)}$$

Here C_i and C_t signify the initial concentration of fluoride ($mg.L^{-1}$) and concentration after time t (min), respectively. The m denotes adsorbent mass per unit volume ($g.L^{-1}$), k is the Langmuir constant and S_s is the specific surface area of adsorbent per unit volume of the reaction mixture (cm^{-1}). β_l stands for the coefficient of external mass transfer ($cm^2\ s^{-1}$). Values of β_l, the coefficient of mass transfer, were calculated at different values of temperature by the slopes and intercepts of the plots of '$\ln [C_t/C_i - 1/(1 + mk)]$ versus t'.

General mechanism thought to be involved in mass transfer is;

I. Gentle movement of pollutant from bulk solution to the upper boundary of adsorbent.

II. Slowly diffusion of adsorbate from boundary film layer to the surface of adsorbent.

III. Adhesion of adsorbate into the internal pore and spaces in between of active sites of adsorbent.

IV. Simultaneous adsorption and desorption of the adsorbate at the active sites of the adsorbent surface.

From above points it can be said that in first step, adsorption might occur in hydro-dynamic conditions that obstruct the concentration gradient in between the solution and boundary film. So, from this point of view, it cannot be a rate limiting step. Hence, external diffusion (step-2) or intra-particle diffusion, will be the slowest step that may be considered as the rate controlling step of proposed adsorption process.

2.7.1.1.4. Diffusion Kinetics (Intra-particle Diffusion Model)

In an ongoing adsorption process, there is an always fair chance of diffusion of adsorbate into the pores of adsorbent which is often considered as rate controlling step of the particular adsorption process. In general, the rate adsorption process will be controlled by the slowest and the rate limiting step. Properties of solute and adsorbent in a batch process are considered as crucial factor to establish the nature of rate limiting steps of any adsorption process. Normally as process is said to be diffusion controlled if rate is dependent upon the rate at which molecules diffuse towards each other. In any adsorption process there is always a possibility of intraparticle diffusion to be involved as rate limiting step and that can be explained by Weber and Morris intra-particle Diffusion Model(Weber and Morris, 1963).

The intraparticle diffusion rate constant (k_{id}) can be determined by the Weber–Morris model that can be expressed as follows:

$$Q_t = K_{id} t^{0.5} + C \qquad \textit{(Eq. 2.12)}$$

where Q_t is the quantity of adsorbate ($mg.g^{-1}$) adsorbed at time t (min), K_{id} is the initial rate of intra particular diffusion calculated by the slope of the plot of Q_t *vs.* $t^{0.5}$ ($mg.L^{-1}.min^{-0.5}$) and C, is the y-intercept which gives proper information all about the boundary layer thickness. Larger the value of C, the greater is the boundary layer effect. This observation was further proved by the value of the intraparticle diffusion coefficient (D_p) and the film diffusion coefficients (D_F) which can be calculated by the following equation.

$$\boldsymbol{D_p = \frac{0.03r^2}{t^{0.5}}} \qquad \textbf{(Eq. 2.13)}$$

$$\boldsymbol{D_F = \frac{(0.23r_0\delta C_s)}{C_L t^{0.5}}} \qquad \textbf{(Eq. 2.14)}$$

Where r (cm) stands for the average radius of the adsorbent particle and $t^{0.5}$ (min) is the time required for completion of half of the adsorption, δ is the film thickness (10^{-3} cm) and C_s and C_L are the concentrations of adsorbate in solid and liquid phase at t=t and t=0 respectively. According to Michelsen *et al.,* if the calculated intra-particle diffusion coefficient (D_p) value be in the range 10^{-11}-$10^{-13}cm^2sec^{-1}$, the intra-particle diffusion will be the rate determining step and, if the calculated film diffusion(D_F) value be in the range of 10^{-6} -$10^{-8}cm^2sec^{-1}$, the rate limiting step will be controlled by film (boundary layer) diffusion (Biswas *et al*., 2009).

2.7.1.1.5. Elovich Model

This equation is more familiar to determine chemisorption kinetics of any gases on heterogeneous surface of any adsorbent (Aharoni and Tompkins, 1970; Allen and Scaife, 1966). Presently, this equation has been widely

applied to evaluate adsorption nature of any adsorbate from aqueous medium. The equation mentioned as follows:

$$\frac{dQ_t}{dt} = a\,exp\,(abQ_t) \qquad \textit{(Eq.2.15)}$$

Where, a signifies the rate of chemisorption at zero coverage (mg/(g/min)) and b is implies the extent of surface occupancy and activation energy required for chemisorption (g/mg). These are obtained from the slope and intercept of the plots of Q_t *vs.* ln (t) (min).

$$Q_t = \frac{1}{b}\,ln(ab) + \frac{1}{b}\,ln\left(1 + \frac{1}{ab}\right) \qquad \textit{(Eq. 2.16)}$$

This equation is the integrated form of Eq. 10 with an assumption that $Q_t = 0$, t = 0 as the lower of limit of integration. If value of t is much higher, i.e. t > 1/ab, the plots of Q_t vs. ln (t) should be linear(Chien and Clayton, 1980; Ranjan *et al*., 2009).

2.7.1.1.6. Richenberg Model

The Richenberg expression can be used to distinguish between the film diffusion and the intra-particle diffusion, which can be given by the following equation(Kumar *et al*., 2005):

$$G = 1 - \frac{6}{\Pi^2}\,exp(-\beta_t) \qquad \textit{(Eq. 2.17)}$$

Where $G = Q_t/Q_e$ and β_t is the mathematical function of G, which can be calculated from respective value of G by the following equation:

$$\beta_t = -0.4977 - ln\left(1 - \frac{Q_t}{Q_e}\right) \qquad \textit{(Eq. 2.18)}$$

The β_t values at different contact times (t) can be calculated using above equation (Eq. 13). The calculated β_t values were plotted against time t (min), and the slope was used for the calculation of factor β_t. The effective diffusion coefficient D_i ($cm^2\ s^{-1}$) has been calculated using the value of factor β_t from following equation.

$$\boldsymbol{\beta_t = \frac{\Pi D_i}{r^2}} \qquad \textit{(Eq. 2.19)}$$

Where adsorbent particles were assumed to be spherical and r is assumed as the radius of the adsorbent particles. The obtained values of D_i will be thus useful to decide the process whether it is intraparticle diffusion or external diffusion. If plots are straight lines passing through the origin, then the adsorption process is governed by particle diffusion mechanisms otherwise, both external diffusion and intraparticle diffusion jointly determine the rate of adsorption(Hamayun *et al*., 2014; Mohammadian *et al*., 2016; Singh *et al*., 2017; Sparks, 1995). Values of film diffusion (D_1) and pore diffusion (D_2) also can provide information regarding the mechanism of adsorption whether it is kinetically influenced by film or pore diffusion. D_1 and D_2 can be determined by the application of following equations(Hamayun *et al*., 2014).

$$\boldsymbol{\frac{Q_t}{Q_e} = 6\left(\left(\frac{D_1}{\Pi a^2}\right)^{0.5}\right)t^{0.5}} \qquad \textit{(Eq. 2.20)}$$

$$\boldsymbol{ln\left(1-\frac{Q_t}{Q_e}\right) = ln\frac{6}{\Pi^2} - \left(\frac{D_2\Pi^2}{a^2}\ t\right)} \qquad \textit{(Eq. 2.21)}$$

D_1 is calculated from the slope of the plot of Q_t/Q_e vs. $t^{0.5}$ and D_2 is calculated from the plots of ln $(1-Q_t/Q_e)$ vs.t for fluoride adsorption on all three proposed adsorbents(Hamayun *et al*., 2014).

2.7.2. Adsorption Isotherm Models

Isotherm modeling of any adsorption process is an essential step to determine the distribution pattern of any adsorbate in between solid and liquid phase at equilibrium. Hence to establish the adsorption efficiency of newly developed adsorbent, optimisation of a particular adsorption study with appropriate isotherm model is considered as basic requirement for commercialization of prepared adsorbate. To achieve the goal of present study, three isotherm models were applied namely; Langmuir, Freundlich and Dubinin- Radushkevich (D-R) isotherms. Langmuir and Freundlich are two basic fundamental isotherm model most widely applied to evaluate equilibrium data of any adsorption process. Meanwhile, D-R isotherm envisaged the nature of adsorption process.

2.7.2.1. Langmuir Isotherm

According to Langmuir model (Clarke and Langmuir, 1916), each adsorbate molecule retains same adsorption energy. All active sites pose equal attraction towards adsorbate and there is no internal interaction in between molecules, hence this isotherm denotes homogeneous, uniform adsorption process. Non-linear form of Langmuir isotherm expressed as follows:

$$\boldsymbol{Q_e = \frac{Q_m K_L C_e}{[1+K_L C_e]}} \qquad \textit{(Eq. 2.22)}$$

Where C_e ($mg.L^{-1}$and Q_e ($mg.g^{-1}$) are the equilibrium fluoride concentration and equilibrium adsorption capacity. The Q_m ($mg.g^{-1}$) is the maximum monolayer adsorption capacity ($mg.g^{-1}$) and K_L ($L.mg^{-1}$) the equilibrium constant related to net enthalpy change of the reaction. Q_m and K_L can be

determined from non-linear analysis of experimental data using the equation (2.22).

2.7.2.2. Freundlich Isotherm

Freundlich model is especially applicable to the non-ideal multilayer adsorption that generally associated with heterogeneous surface of adsorption sites indicating that the binding sites are not equivalent and /or independent (Freundlich, 1906). The non-linear expression of Freundlich can be set as,

$$\boldsymbol{Q_e = K_F \times C_e^{1/n}} \qquad \textit{(Eq. 2.23)}$$

Where, the K_F is the Freundlich adsorption capacity and 1/n is an empirical constant related to the adsorption intensity. Both K_F and n can be obtained from non-linear analysis of experimental data using the equation (2.23).

2.7.2.3. Dubinin - Radushkevich (D-R) Isotherm

Dubinin-Radushkevich (D–R) isotherm was elucidated to estimate the free energy of reaction and can be obtained from the equilibrium isotherm data to predict the nature of adsorption(Dubinin, M.M. and Radushkevich, 1947). Linear form of this isotherm is written as:

$$\boldsymbol{lnQ_e = lnQ_m - \beta\varepsilon^2} \qquad \textit{(Eq. 2.24)}$$

Where ε the Polanyi potential is can be extracted from the equation (2.25) below,

$$\varepsilon = \boldsymbol{RT\ ln\left(1 + \frac{1}{C_e}\right)} \qquad \textit{(Eq. 2.25)}$$

The plots of the ln Q_e against ε^2 become a straight line and the values of slope and intercept of the plot was used to calculate the value of β and Q_m. Q_e and

Q_m are equilibrium and maximum D-R adsorption capacities in (mol. kg^{-1}), respectively, and β is signifying activity coefficient mainly related with the mean free energy (E_{DR}) of reaction as per the following equation:

$$\boldsymbol{E_{DR} = 1/(-2\beta)^{1/2}} \qquad \textit{(Eq. 2.26)}$$

This adsorption potential is independent of the temperature, but it varies depending on the nature of adsorbent and adsorbate. The mean free energy of adsorption provides information about the adsorption mechanism. Depending on the obtained value of E_{DR}, an adsorption process can be categorised in three types such as (i) physisorption if E_{DR} = 8.0 kJ mol^{-1}, (ii) ion-exchange if E_{DR} = 8.0–16.0 kJ mol^{-1} and (iii) chemisorption if E_{DR}> 16.0 kJ mol^{-1} (Ghosh *et al*., 2014; Mukhopadhyay *et al*., 2017; Saha *et al*., 2016).

2.7.3. Thermodynamics Studies

Study of different thermodynamic parameters such as standard free energy (ΔG^0), standard enthalpy (ΔH^0) and standard entropy (ΔS^0) changes used for evaluate thermodynamic feasibility of the adsorption process and implication of Gibb's free energy change associated with reaction process (Biswas *et al*., 2009; Mukhopadhyay *et al*., 2017). These parameters generally calculated as per following equations:

$$\boldsymbol{\Delta G° = \Delta H° - T\Delta S°} \qquad \textit{(Eq. 2.27)}$$

$$\boldsymbol{\Delta G° = -2.303RT\, log K_c} \qquad \textit{(Eq.2.28)}$$

From equations ***Eq. 2.27*** and ***Eq.2.28*** equation ***Eq.2.29*** could be derived,

$$\log K_c = \frac{\Delta S^\circ}{2.303R} - \left(\frac{\Delta H^\circ}{2.303R}\right)\frac{1}{T} \qquad \textit{(Eq.2.29)}$$

Where K_c is the equilibrium constant at temperature T, and K_c was calculated as

$$K_c = \frac{Q_e}{C_e} \qquad \textit{(Eq.2.30)}$$

Q_e (mg.L^{-1}) represents equilibrium adsorbate concentration, C_e is concentration of adsorbate in bulk solution in equilibrium (mg.L^{-1}). Q_e/C_e is called the adsorption affinity, which is the ratio of the amount adsorbed per unit mass (Q_e) to the solute concentration in solution (C_e) at equilibrium. Assuming ΔH^0 and ΔS^0 to be constant within the temperature range studied, the values may be calculated from the slope and the intercept of the straight line obtained from the plot of log K_c versus 1/T and ΔG^0, the change of free energy, at various temperatures are calculated from the above equation (Eq.2.27).

2.7.4. Activation Energy

The change of values of the rate constant with increase in temperature may be described by the Arrhenius equation and can be expressed as

$$k_2 = A\, exp\left(-{}^{E_a}/_{RT}\right) \qquad \textit{(Eq.2.31)}$$

Here, K_2 is meant as the rate constant of pseudo-second order kinetic model (g.mg^{-1}.min^{-1}), A (g.mg^{-1}.min^{-1}), is a temperature independent factor and E_a (KJ mol^{-1}) is the activation energy of any particular reaction. R and T are well known and mentioned earlier. Logarithm of above equation can be

demonstrated by a linear relationship of Arrhenius equation and can be represented as below;

$$\boldsymbol{ln\, k_2 = ln\, A + \left(-{}^{E_a}/_{R}\right)\frac{1}{T}} \qquad \textit{(Eq.2.32)}$$

the plot of ln k_2 against 1/T, will be a straight-line and from the slope ($-E_a/R$) of straight line the value of activation energy may be calculated (Laidler, 1984).

2.8. Fixed Bed Column Adsorption Models

2.8.1. Thomas Model

Data acquired from continuous column operation was used to calculate maximum solid phase concentration of any adsorbent on fixed bed column and adsorbent rate constant using the kinetics model developed by Thomas model (Thomas, 1944). Thomas model is the most common and general widely used model to evaluate column operation performance. The mathematical expression of Thomas model for any adsorption column is given as follows:

$$\boldsymbol{ln\left(\frac{C_i}{C_t} - 1\right) = \frac{K_{th} Q_0 w}{v} - K_{th} C_i t} \qquad \textit{(Eq. 2.33)}$$

Where, k_{Th} (mL.min^{-1}.mg^{-1}) is the Thomas rate constant; Q_0 (mg.g^{-1}) is the equilibrium uptake capacity per g of the adsorbent; C_i (mg.L^{-1}) is the influent concentration; C_t (mg.L^{-1}) is the effluent concentration at time t; W (g) the mass of adsorbent and V (mL.min^{-1}) is the flow rate. The value of C_t/C_i is the ratio of effluent and influent concentrations.

2.8.2. Bed Depth Service Time (BDST) Model

This model is originally developed by Hutchins based on physically measuring the capacity of the fixe deb at different breakthrough values. This simplified model form was developed with an assumption that the intraparticle mass-transfer resistance and external film resistance are negligible, means the adsorbate is adsorbed only on the surface of the adsorbent (Hutchins and A., 1973). This can be expressed as;

$$t_b = \left(\frac{DN_{BD}}{C_i v}\right) - \frac{1}{K_{BD}C_i}\ln\left(\frac{C_i}{C_b} - 1\right) \quad \textit{(Eq. 2.34)}$$

$$t_b = mD - K \quad \textit{(Eq. 2.35)}$$

$$m = \left(\frac{N_{BD}}{C_i v}\right) \quad \textit{(Eq.2.36)}$$

$$K = -\left[\frac{1}{K_{BD}C_i} ln\left(\frac{C_i}{C_b} - 1\right)\right] \quad \textit{(Eq. 2.37)}$$

$$D_o = \frac{v}{K_{BD}N_{BD}} ln\left(\frac{C_i}{C_b} - 1\right) \quad \textit{(Eq. 2.38)}$$

Where, t_b is the service time at breakthrough point, N_{BD} is the adsorption capacity per unit volume of bed ($mg.cm^{-3}$), and D is the depth of the adsorbent bed (cm). C_i and C_b are the concentrations ($mg.L^{-1}$) of adsorbate in the feed solution and at the breakthrough point, respectively; v is the flow rate ($mL.\ min^{-1}$) of effluent; and K_{BD} ($L.mg^{-1}.min^{-1}$) is the rate constant of adsorption reaction. (Eq. 2.34) can be reframed in the form where m is the slope of the BDST line ($m= N_{BD}/C_iV$) and K is the intercept of this equation thus, N_{BD} and K_{BD} can be evaluated from the slope (m) and intercept (K), respectively, of a plot t_b versus D.

2.8.3. Statistical Model

2.8.3.1. Artificial Nneural Network (ANN) Modeling

An artificial neural network (ANN) is well known but simplified computational and statistical model that is vaguely inspired by the structure of biological neural networks. ANN is established framework that can effectually classify the patterns and extract trends from inaccurate and complicated non–linear data. This intrinsic property of ANN model made it one of the authentic method suitable for prediction and assessment of a given system and to predict, analyse and design the existing complex non–linear adsorption properties (Ayodele *et al*., 2017; Giri *et al*., 2011; Nasr *et al*., 2012; Raj *et al*., 2013; Shi *et al*., 2017). It is used as a very powerful tool to understand the nature of a new processes (Cavas *et al*., 2011).Among existing forms of ANN architecture, multilayer–perception (MLP) is accepted widely to understand the behaviour of chemical process particularly (Pandharipande and Deshmukh, 2013; Turp *et al*., 2011). In general, artificial neurons are amassed into layers. Different layers are actively do perform different kinds of conversions based on the connectionist approach on their inputs. Signals travel from the first layer-the input layer to the last layer - the output layer after criss-crossing the layers multiple times without knowing the intricate relationship among them (Ghaedi and Vafaei, 2017). Each of these layers consists of a number of inter–connected processing units known as neurons (Aghav *et al*., 2011; Roy *et al*., 2013; Shi *et al*., 2017). The interaction between these neurons are circulated by imposing signals to one–another along weighted connections. Every neuron is connected to other neurons in the previous and succeeding layer by links. The input layer response first with receiving information from external sources

and this information is then transmitted to the hidden layer for processing. However, the input values are weighted discretely just prior to the inflowing into the hidden layer (Roy *et al.*, 2013). The hidden layer then accomplishes all the data processing and produces output based on the sum of the weighted values from the input layer modified by a sigmoid transfer function (f).The output from a neuron in the output layer can be obtained by using the following empirical formula:

$$\boldsymbol{O_i = f \sum_{j=0}^{n} W_{ij} O_j} \qquad \textbf{(Eq. 2.39)}$$

Where n signifies the number of inputs, O_j is the j^{th} input to the neuron, W_{ij} represents the connection weight between the j^{th} hidden neuron to i^{th} output neuron and *f* is the sigmoid transfer function. In present research, a tan–sigmoid transfer function (tan–sig) at hidden layer and a linear transfer function (purelin) at output layer were used. Furthermore, for network training back–propagation algorithm was also applied. The tan–sigmoid transfer function is expressed as:

$$\boldsymbol{\int(x) = \frac{2}{1+e^{-2x}} - 1} \qquad \textbf{(Eq. 2.40)}$$

Where f(x) represents hidden neuron output. The Levenberg– Marquardt back–propagation algorithm was applied for network training (Chowdhury *et al*., 2013). For batch adsorption study, the input factors to the ANN model were pH, initial fluoride concentration, adsorbent dose, contact time and temperature whereas the percentage removal or both the removal and uptake capacity were considered as outputs. For column study, the input

factors to the ANN model were bed height, initial fluoride concentration, flow rate and breakthrough volume and exhaust volume were considered as output. Here, all ANN calculations and graphical presentations were carried out using neural network toolbox of Neuro solution 5(R) or SPSS–17 statistical software.

2.8.3.2. Response Surface Methodology (RSM)

Response surface methodology (RSM) is an empirical statistical technique introduced by George E. P. Box and K. B. Wilson in 1951 usually employed for multiple regression analysis to explore the relationships between several descriptive variables and one or more response variables. The first step of RSM is to focus on the optimum operating conditions for any given experimental system with additional appropriate approximation, with the purpose of finding a true relationship between the set of independent variables (factors) and the dependent variable i.e., the response. Central composite design (CCD), Box–behnken statistical experiment design (BBD), (and two–level full factorial design (FFD) are the most widely accepted RSM techniques used by research for interpretation of experimental data (Roy, 2014). Among them, CCD is considered as most useful tool for building up a second order (quadratic) model for the response variable without requiring to use a complete three-level factorial experiment. The relationship between desired response and independent variables can be written as:

$$\boldsymbol{Y = f(X_1, X_2, X_3, \ldots, X_n) + \epsilon} \qquad \textit{(Eq. 2.41)}$$

where *Y* denotes the response, *X* are independent variables, *n* is the number of factors being studied and *ε* is experimental error. Following equation also applicable to find out coded values of process variables;

$$\boldsymbol{Coded\ value = X_i = \frac{X_i - X_0}{\Delta X} (i = 1, 2, 3, 4, \ldots . K)} \qquad \textit{(Eq. 2.42)}$$

Where X_i, the dimensionless value of a process variable and the real value of the ith factor of an independent variable, $X_0$is the value of Xi at the centre point and ΔX denotes the step change. A second order polynomial regression model equation has been applied to get true functional relationship between independent variables and the response and also to define the effect of variables in terms of linear, quadratic and cross product terms.

$$\boldsymbol{Y = \beta_0 + \sum_{i=0}^{n} \beta_i X_i + \sum_{i=0}^{n} \beta_{ii} X_{ii}^2 + \sum_{i,j=1(i \neq j)}^{4} \beta_{ij} X_i X_j + \varepsilon}$$

(Eq. 2.43)

Where Y= predicted response, β_0= offset term, β_i=linear effect, β_{ii} = squared effect, β_{ij}=interaction effect. For four independent variables, Equation 2.43 can be written as in the following equation with Y as ultimate response in their coded values.

$$\boldsymbol{Y = \beta_0 + \beta_1 X_1 + \beta_2 X_2 + \beta_3 X_3 + \beta_4 X_4 + \beta_{12} X_1 X_2 + \beta_{13} X_1 X_3 + \beta_{14} X_1 X_4 + \beta_{23} X_2 X_3 + \beta_{24} X_2 X_4 + \beta_{34} X_3 X_4 + \beta_{11} X_1^2 + \beta_{22} X_2^2 + \beta_{33} X_3^2 + \beta_{44} \ldots \ldots \ldots \ldots \ldots}$$

(Eq. 2.44)

CCD design consist of a 2^n factorial runs (coded to the usual ± notation), 2n axial runs (± α, 0, 0 ...., 0), (0, ± α, 0 ....., 0),..... (0, 0 ....., ±α) and n_c centre runs (6 replicates, 0, 0, 0 ...., 0). The number of factors n increases the number of runs for a complete replicate of the design which is expressed as follows:

$$\boldsymbol{N = 2^n + 2n + n_c} \qquad \textit{(Eq. 2.45)}$$

In the present research work, a set of three independent variables, likely initial fluoride concentration, flow rate, and bed depth height were taken and their impact on the response variable i.e. breakthrough time for continuous fixed–bed adsorption were extensively studied using CCD model with the help of Design–Expert (7.0.3) software. The range of α lies between 1 and √n. for assessment of the capability of the developed model, the exploration of variance (ANOVA) was done to describe the coefficients of the quadratic equation. Significance of the process variables was checked by *p*–value and *F*–value (Roy, 2014; Roy *et al*., 2014, 2013).